Supplementary Information for

Redox-Active Triazatruxene-based Conjugated Microporous Polymers for High-Performance Supercapacitors

Xiangchun Li,[a] Yizhou Zhang,[a,b] Chunyu Wang,[a] Yi Wan,[a] Wen-Yong Lai,*[,a,b] Huan Pang,*[,c] and Wei Huang*[,a,b]

[a] Key Laboratory for Organic Electronics and Information Displays (KLOEID), Institute of Advanced Materials (IAM), Jiangsu National Synergetic Innovation Center for Advanced Materials (SICAM), Nanjing University of Posts & Telecommunications, 9 Wenyuan Road, Nanjing 210023, China

[b] Key Laboratory of Flexible Electronics (KLOFE), Institute of Advanced Materials (IAM), Jiangsu National Synergetic Innovation Center for Advanced Materials (SICAM), Nanjing Tech University (Nanjing Tech), 30 South Puzhu Road, Nanjing 211816, China

[c] College of Chemistry and Chemical Engineering, Yangzhou University, Yangzhou, Jiangsu 225002, China

*Correspondence and requests for materials should be addressed to W.-Y. L. (email: iamwylai@njupt.edu.cn) or to H. P. (email: huanpangchem@hotmail.com) or to W. H. (email: wei-huang@njtech.edu.cn).

1. Experimental details and characterizations

All the reagents used were purchased from Sigma-Aldrich, J&K or Xiya Reagent (China). When necessary, solvents and reagents were purified using standard procedures. Materials Synthesis: **TATR** were synthesized as described previously.[1] All manipulations involving air-sensitive reagents were performed under an atmosphere of dry nitrogen. Described below are the synthesis and purification procedures for the key intermediates and final products.

Characterization of materials: NMR spectra were recorded on a Bruker Ultra Shield Plus 400 MHz NMR (^{1}H: 400 MHz, ^{13}C: 100 MHz). The matrix assisted laser desorption ionization time of flight mass spectroscopy (MALDI-TOF MS) measurements were carried out with a Shimadzu AXIMA-CFR mass spectrometer. Scanning electron microscopy (SEM) observation was carried out using a JEOL 6340-FESEM system operated at 3 kV. Transmission electron microscopy (TEM) was performed on a JEOL JEM-3010x operated at 100 kV. TEM samples were prepared by first dispersing the materials into ethanol or toluene assisted by ultrasonication. A drop of as-prepared solution was cast onto a holey carbon film of a copper TEM grid for examination.

X-ray diffraction (XRD): The powder wide-angle X-ray diffraction (WAXD) measurements were carried out with a Bruker D8 Advance diffractometer with Cu radiation (λ_1 = 1.54056 Å, λ_2 = 1.54439 Å) at 40 kV and 40 mA equipped with a Linkseye detector. Measurements were collected within a 2θ range from 3 to 40° with a step size of 0.2°.

Nitrogen sorption analysis: The pore structure of conjugated microporous polymer sample was assessed from the N_2 isotherm curve measured by a gas adsorption analyzer (V-Sorb 2800P, Gold APP Corp., Beijing, China). Prior to the adsorption experiments, all samples were degassed at 150 °C for 3 h to eliminate the surface contaminants (water or oils). The Brunauer-Emmett-Teller (BET) method was utilized to calculate the specific surface areas and the Saito-Florey (SF) method

for the calculation of pore size.

X-ray photoelectron spectroscopy (XPS): The XPS analysis was performed on ESCL AB250 system with monochromatic Al Kα excitation under vacuum below $1*10^{-7}$ Pa. The sample was tested on Pt net electrode without any additive.

Electrochemical analysis: Electrochemical studies on all the electrodes were conducted in a three electrode system: Electrochemical studies on the as-prepared electrodes were carried out on a CHI 660D electrochemical working station (Shanghai Chenhua Instrument, Inc.). All electrochemical performances were carried out in a conventional three-electrode system equipped with a platinum electrode and a saturated calomel electrode (SCE) as counter and reference electrodes, respectively. Before electrochemical measurements, we have purged out O_2 from the solution by the inert gas-Ar. The working electrode was made by mixing active materials, acetylene black, and PTFE (polytetrafluoroethylene) at a weight ratio of 80:15:5, coating on a piece of nickel foam of about 1 cm^2, and being pressed to be a thin foil at the pressure of 5.0 MPa. The electrolyte was 1.0 M Na_2SO_4 solution. Cyclic voltammetric (CV) measurements were recorded from -1.0 to 0 V with a scan rate from 5 to 50 mV s^{-1}. Galvanostatic charge-discharge measurements were performed at different constant current densities from 1.0 to 10 A g^{-1}.

The specific capacitance (C_s, F g^{-1}) was calculated from the slope of discharge curve using the equation of $C_s = I*t/(V * m)$, where I is the discharge current in the unit of A, V is the discharge voltage in the unit of V, t is the discharge time in the unit of s, and m is the mass of **TAT-CMP-1** or **TAT-CMP-2** in the film electrode in the unit of g.

1.1. Synthesis of 5,10,15-trihexyl-3-nitro-10,15-dihydro-5H-diindolo[3,2-a:3',2'-c] carbazole (**TAT-3NO$_2$**). 65% nitric acid (1.5 mL, 33.3 mmol) was added to a solution of **TATR** (3.68 g, 6.2 mmol) in dichloromethane (DCM) (37 mL) at 0 °C. The resulting mixture was stirred for 4 h and

then extracted with DCM (100 mL) for three times. The organic layer was dried with anhydrous magnesium sulfate ($MgSO_4$) and evaporated to dryness. The residue was purified on a silica gel column eluted with DCM: Petroleum Ether (PE) (1:1) to afford **TAT-3NO$_2$** (3.73 g) in 82%. ^{1}H NMR (400 MHz, $CDCl_3$, ppm): δ 8.58 (s, 3H), 8.30 (s, 6H), 5.02-4.93 (m, 6H), 1.99 (s, 6H), 1.29-1.22 (m, 18H), 0.80 (t, J = 6.7 Hz, 9H); ^{13}C NMR (100 MHz, $CDCl_3$, ppm): δ 143.82, 142.47, 139.68, 127.55, 121.10, 116.15, 107.00, 103.38, 47.65, 31.94, 31.23, 29.95, 29.71, 29.37, 26.22, 22.70, 22.38, 14.13, 13.84; MALDI-TOF MS (*m/z*): Calcd for $C_{42}H_{48}N_6O_6$, Exact Mass: 732.36, Mol. Wt.: 732.88, Found: 731.090 (M^+); Elemental analysis calcd (%): C 68.83, H 6.60, N 11.47. Found: C 68.72, H 6.33, N 11.78.

1.2 Synthesis of 5,10,15-trihexyl-10,15-dihydro-5H-diindolo[3,2-a:3',2'-c]carbazol-3-amine (**TAT-3NH$_2$**). Under nitrogen, **TAT-3NO$_2$** (1.04 g, 1.60 mmol) and palladium on activated carbon (Pd/C) (0.14 g) were dissolved in *N*,*N*-dimethyl formamide (20 mL) and the solution was refluxed. Hydrazine monohydrate (1.5 mL) was added dropwise, and the mixture was stirred at this temperature for 10 h. Pd/C was removed by filtration through Celite and the filtrate was extracted with DCM. The organic layer was dried with Na_2SO_4 and the solvents were evaporated under vacuum. The crude product was purified on a silica gel column using DCM/PE: 1/4, as eluent to get **TAT-3NH$_2$** (0.75 g) in 73%. ^{1}H NMR (400 MHz, $CDCl_3$, ppm): δ 7.99 (d, J = 8.5 Hz, 3H), 6.87 (d, J = 2.0 Hz, 3H), 6.70 (dd, J = 8.5, 2.0 Hz, 3H), 4.75-4.69 (m, 6H), 3.84 (s, 6H), 1.93 (s, 6H), 1.27 (t, J = 11.0 Hz, 18H), 0.83 (d, J = 7.0 Hz, 9H); ^{13}C NMR (100 MHz, $CDCl_3$, ppm): δ 142.92, 142.85, 141.21, 141.06, 138.33, 138.02, 123.53, 123.52, 122.60, 122.39, 121.55, 121.52, 119.45, 119.42, 116.49, 110.47, 110.29, 109.27, 103.60, 103.50, 103.16, 96.79, 47.14, 47.09, 46.80, 31.51, 31.49, 31.48, 29.87, 29.76, 29.75, 29.55, 26.40, 22.54, 22.53, 22.51, 13.97, 13.95; MALDI-TOF MS (*m/z*): Calcd for $C_{42}H_{54}N_6$, Exact Mass: 642.44, Mol. Wt.: 642.94, Found: 642.55 (M^+); Elemental

analysis calcd (%): C 78.46, H 8.47, N 13.07. Found: C 78.64, H 8.37, N 13.02.

1.3 Synthesis of **TAT-CMP-1**. A 25 mL Schlenk tube (OD26 x L110 mm) was charged with Pyromellitic dianhydride (**PMDA**) (32.7 mg, 0.15 mmol) and **TAT-3NH$_2$** (64.2 mg, 0.1 mmol) in a 1/2 v/v solution (6 mL) of 1,4-dioxane/mesitylene. The tube was sonicated for 5 min and flash frozen at 77 K (LN_2 bath), evacuated to an internal pressure of 0.15 mmHg and then tightened by the screw cap. The reaction mixture was heated at 120°C for 3 d to afford a brown precipitate, which was isolated by filtration over a medium glass frit and washed with anhydrous 1,4-dioxane. The product was immersed in anhydrous DCM (20 mL) for 3 d. In this process, the activation solvent was decanted and freshly replaced for four times. The solvent was removed under vacuum at room temperature to get **TAT-CMP-1** (75.0 mg) in 82%. Elemental analysis calcd (%): C 71.11, H 5.35, N 8.65. Found: C 70.82, H 5.51, N 8.54.

1.4 Synthesis of **TAT-CMP-2**. A 25 mL Schlenk tube (OD26 x L110 mm) was charged with Terephthalaldehyde (**TPAL**) (20.1 mg, 0.15 mmol) and **TAT-3NH$_2$** (64.2 mg, 0.1 mmol) in a 1/2 v/v solution (6 mL) of 1,4-dioxane/mesitylene. The tube was sonicated for 5 min and flash frozen at 77 K (LN_2 bath), evacuated to an internal pressure of 0.15 mmHg and then tightened by the screw cap. The reaction mixture was heated at 120°C for 3 d to afford a red precipitate, which was isolated by filtration over a medium glass frit and washed with anhydrous 1,4-dioxane. The product was immersed in anhydrous DCM (20 mL) for 3 d, during which the activation solvent was decanted and freshly replaced for four times. The solvent was removed under vacuum at room temperature to get **TAT-CMP-2** (67.1 mg) in 85%. Elemental analysis calcd (%): C 80.72, H 7.47, N 10.05. Found: C 80.43, H 7.13, N 10.40.

2. Supporting figures and tables

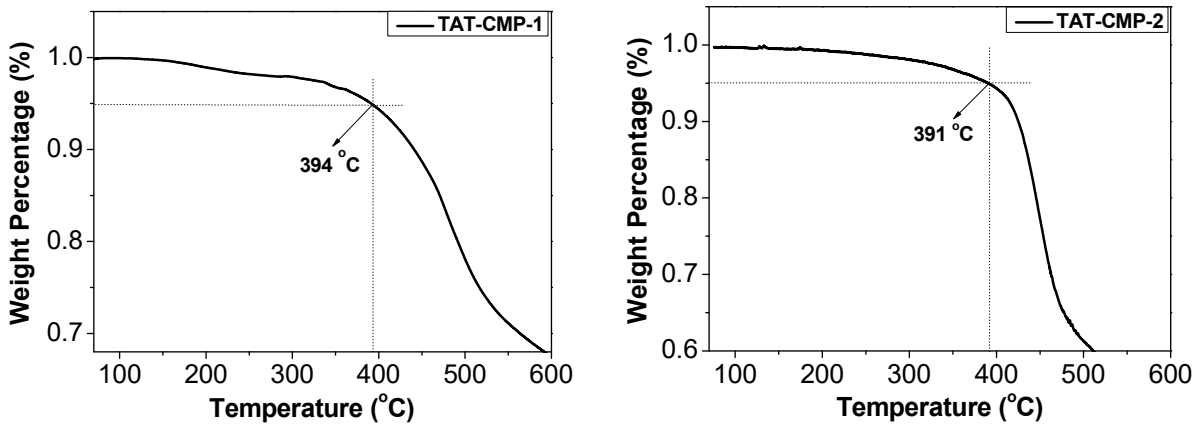

Figure S1. TGA thermograms of **TAT-CMP-1** (left) and **TAT-CMP-2** (right) measured at a heating rate of 10 °C min^{-1}.

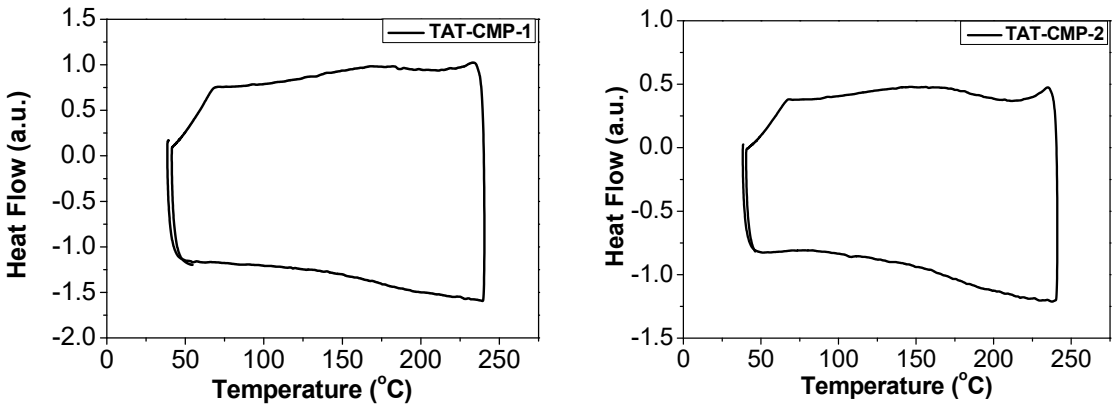

Figure S2. DSC thermograms of **TAT-CMP-1** (left) and **TAT-CMP-2** (right) measured at a heating rate of 10 °C min^{-1}.

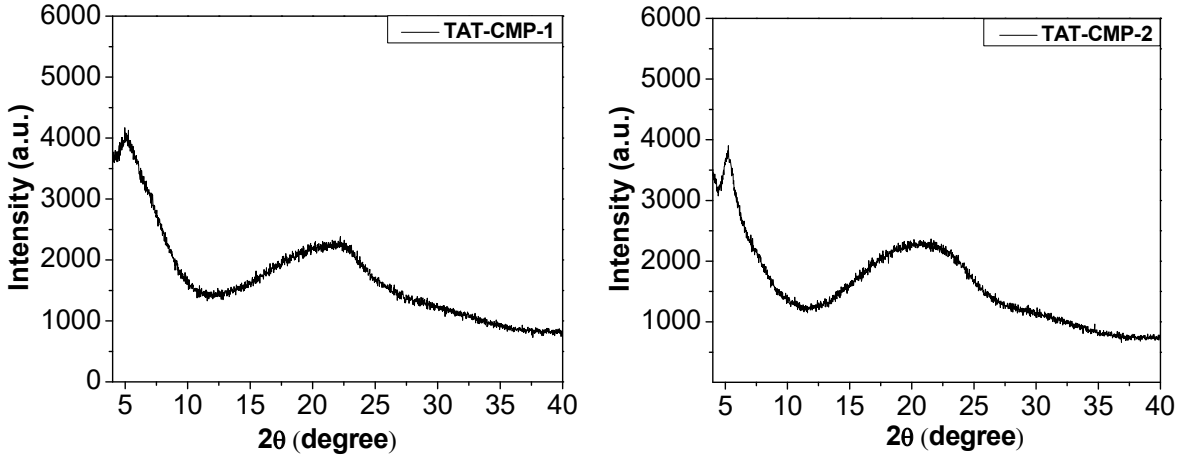

Figure S3. The powder XRD patterns of **TAT-CMP-1** and **TAT-CMP-2**.

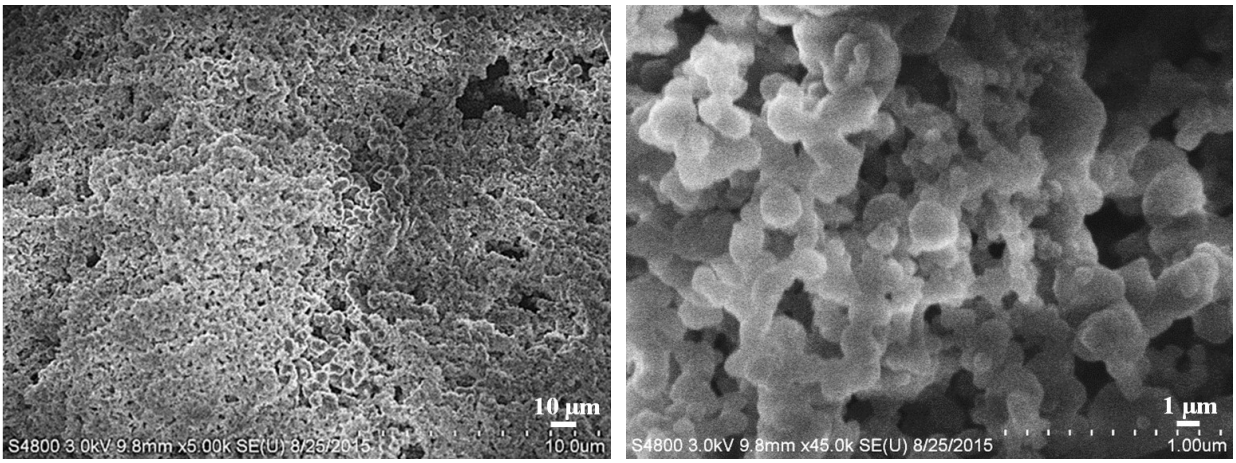

Figure S4. SEM images of **TAT-CMP-1**.

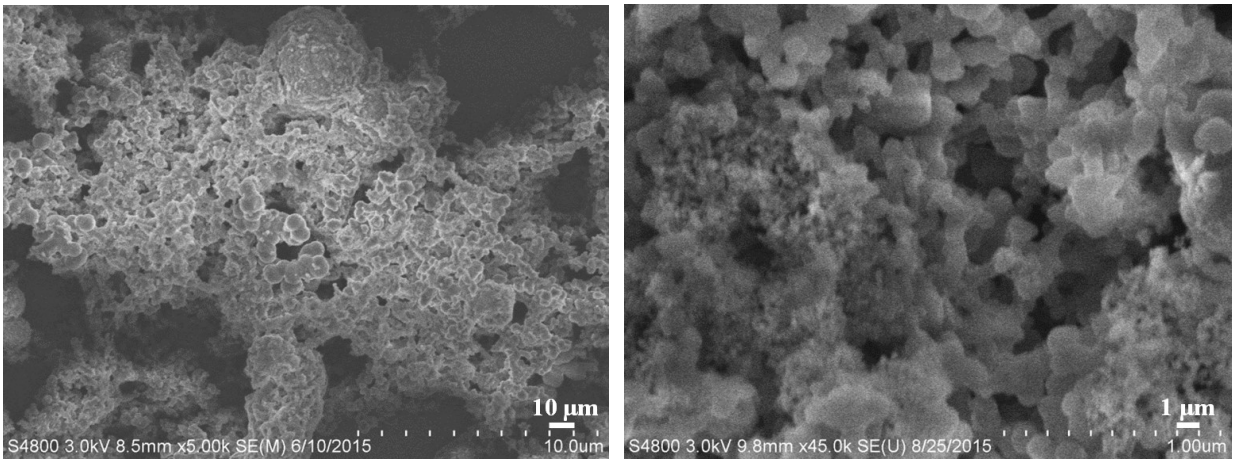

Figure S5. SEM images of **TAT-CMP-2.**

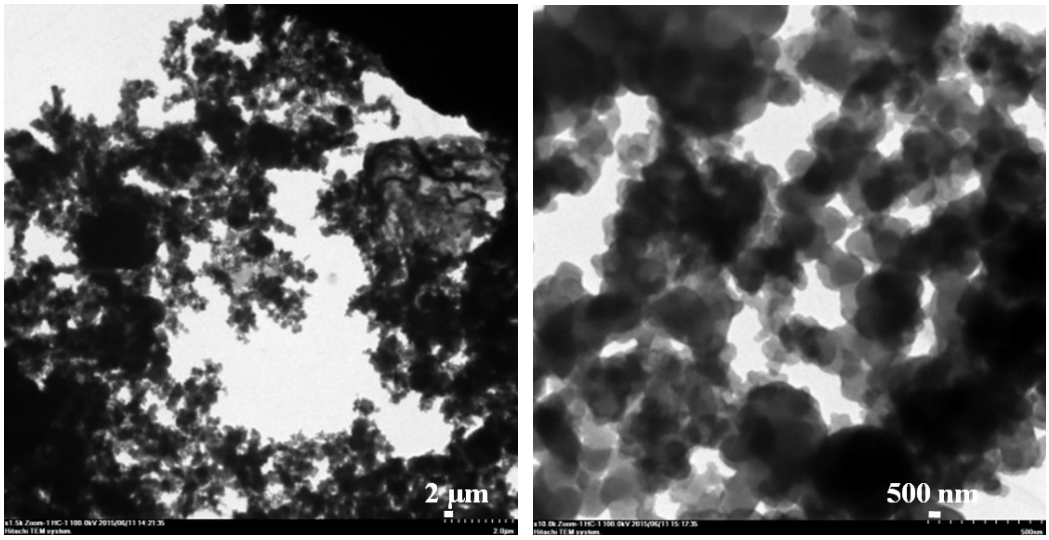

Figure S6. TEM images of **TAT-CMP-1.**

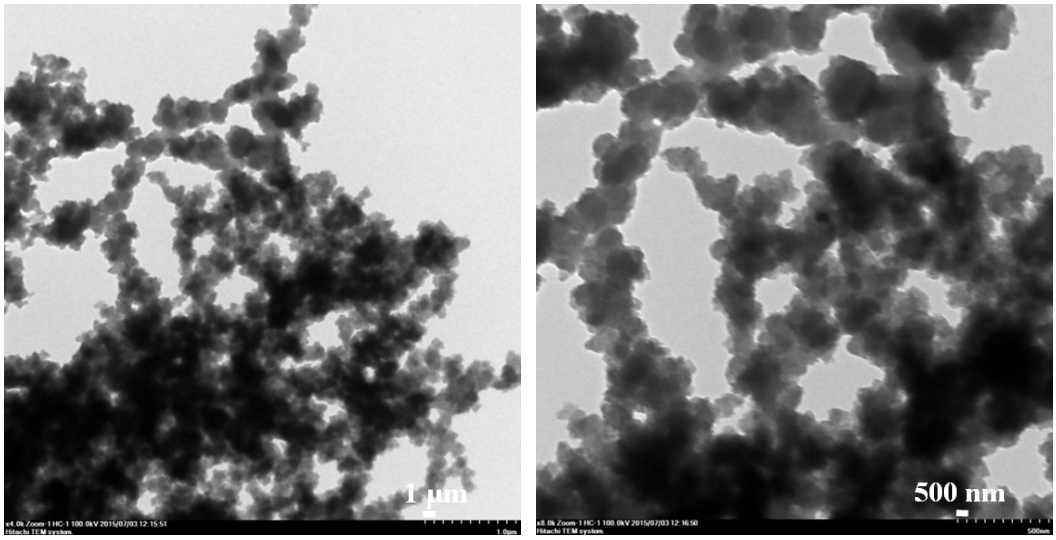

Figure S7. TEM images of **TAT-CMP-2.**

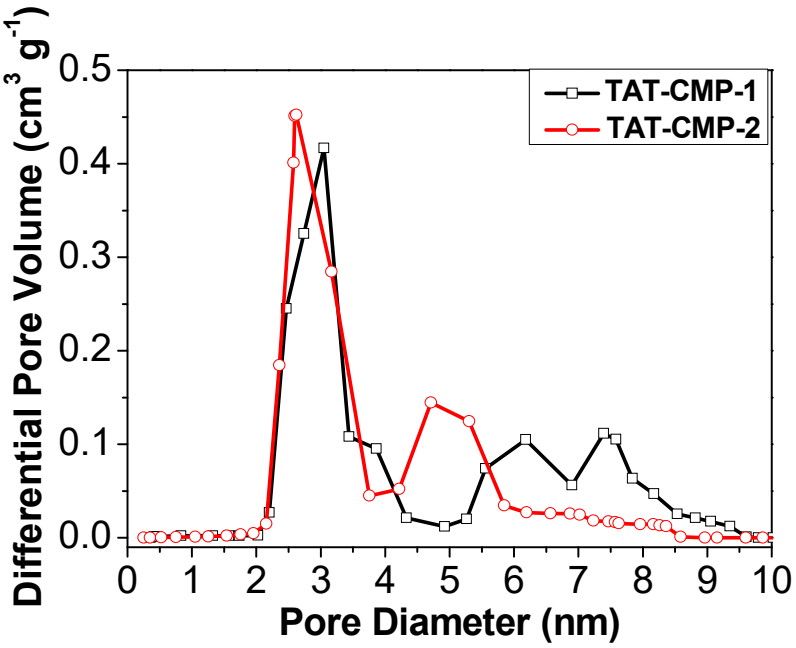

Figure S8. The average pore distribution of **TAT-CMP-1** and **TAT-CMP-2.**

Table S1. The peak of N 1s of **TAT-CMP-1** and **TAT-CMP-2** in the sencond CV scanning at different potentials.

		N 1s Scan A (eV)	N 1s Scan B (eV)	N 1s Scan C (eV)	N 1s Scan D (eV)
TAT-CMP-1	Before CV scanning	400.2	401.1	403.0	--
	-0.5-0 V	400.2	--	403.0	--
	-1.0-0 V	400.3	--	--	--
	-1.5-0 V	400.3	--	--	--
	-2.0-0 V	400.3	--	--	--
TAT-CMP-2	Before CV scanning	398.7	399.9	402.7	401.5
	-0.5-0 V	398.8	399.9	402.6	--
	-1.0-0 V	399.9	398.9	--	--
	-1.5-0 V	399.8	398.7	--	--
	-2.0-0 V	399.9	398.7	--	--

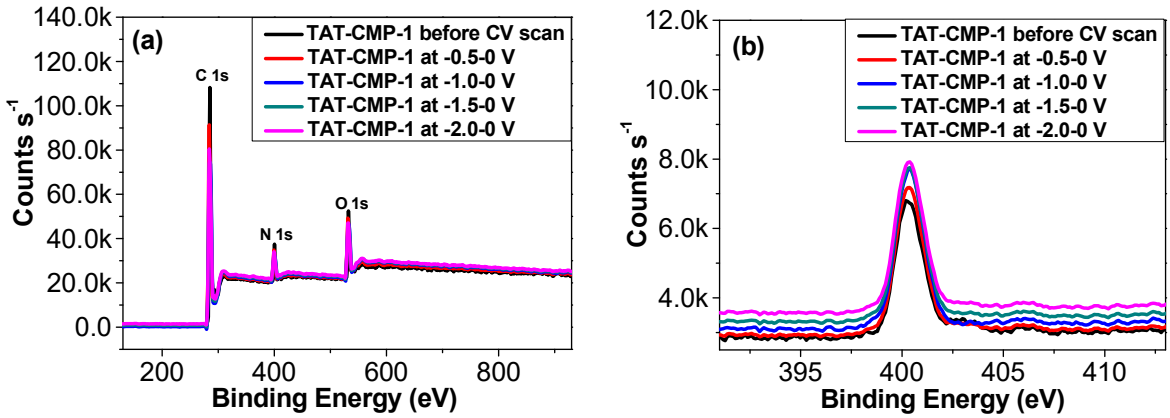

Figure S9. (a) XPS spectra of **TAT-CMP-1** recorded in the second CV scanning at different potentials from 0 V to -0.5 V, -1.0 V, -1.5 V, and -2.0 V; (b) N 1s core-level spectra of **TAT-CMP-1** recorded in the second CV scanning from 0 V to -0.5 V, -1.0 V, -1.5 V, and -2.0 V.

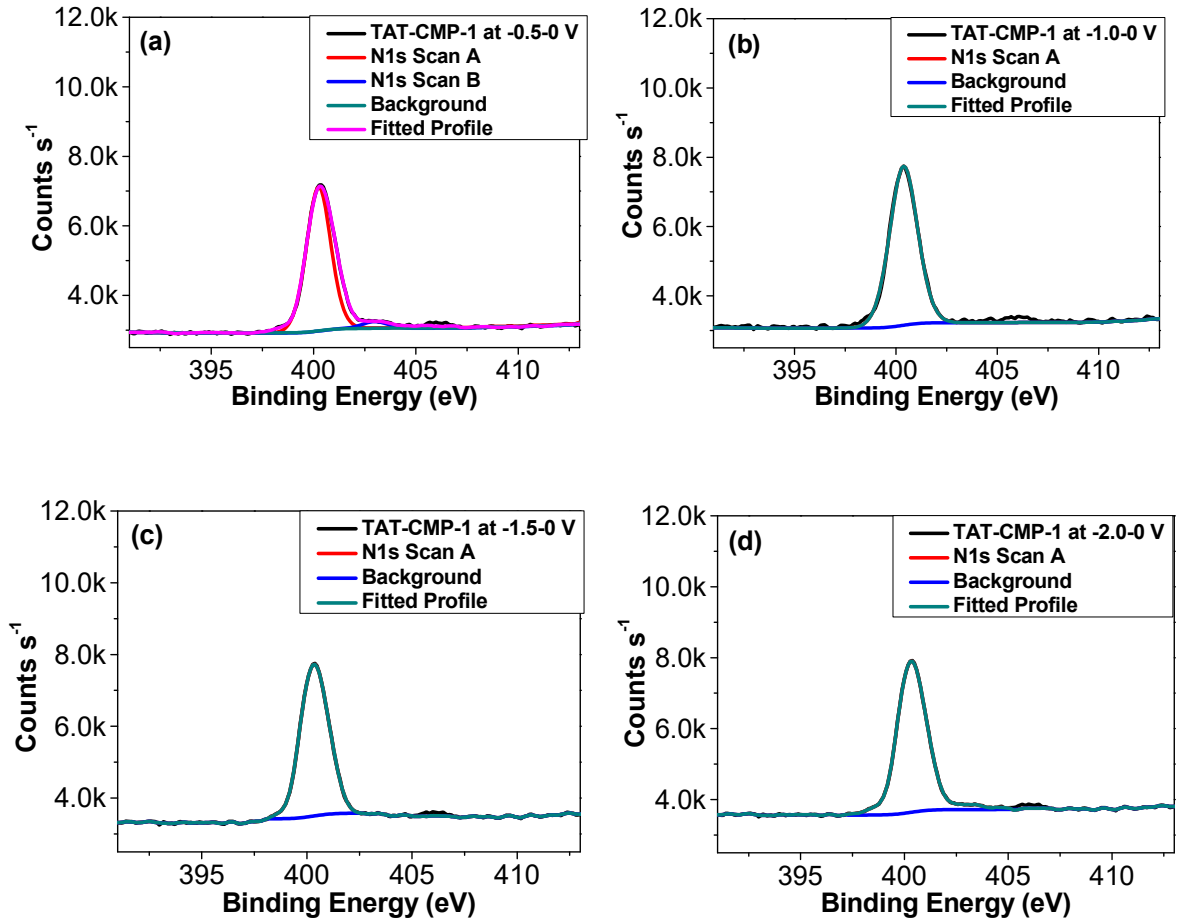

Figure S10. N 1s core-level spectra of **TAT-CMP-1** recorded in the second CV scanning at different potentials from 0 V to (a) -0.5 V, (b) -1.0 V, (c) -1.5 V, and (d) -2.0 V.

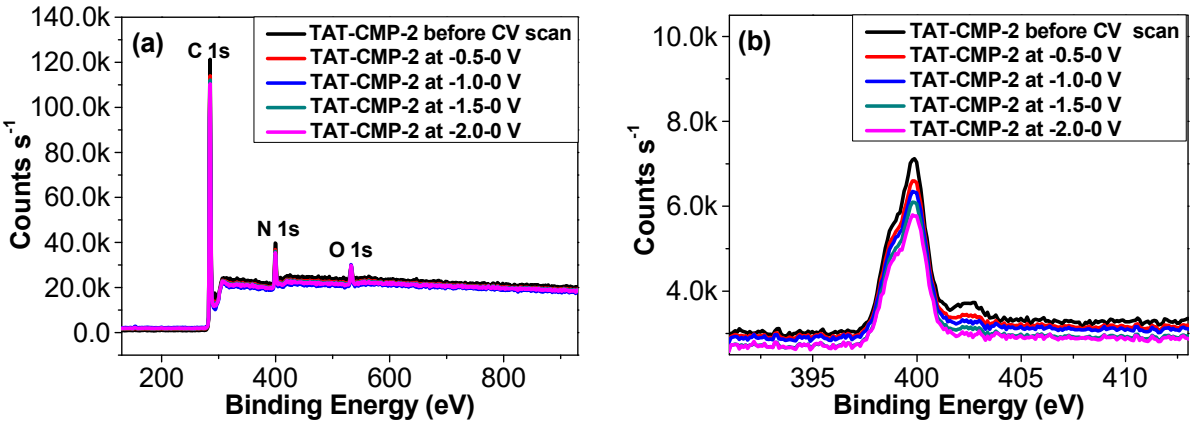

Figure S11. (a) XPS spectra of **TAT-CMP-2** recorded in the second CV scanning at different potentials from 0 V to -0.5 V, -1.0 V, -1.5 V, and -2.0 V. (b) N 1s core-level spectra of **TAT-CMP-2** recorded in the second CV scanning from 0 V to -0.5 V, -1.0 V, -1.5 V, and -2.0 V.

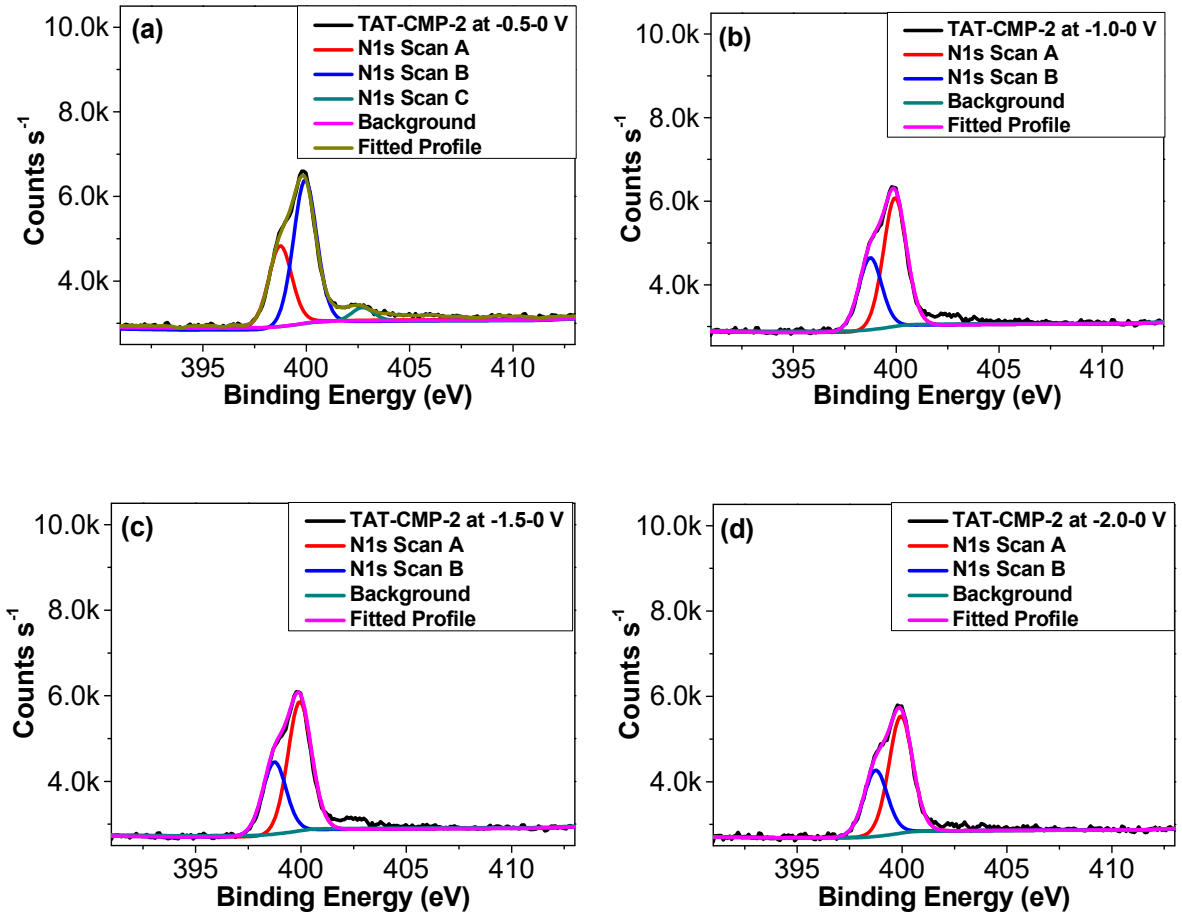

Figure S12. N 1s core-level spectra of **TAT-CMP-2** recorded in the second CV scanning at different potentials from 0 V to (a) -0.5 V, (b) -1.0 V, (c) -1.5 V, (d) -2.0 V.

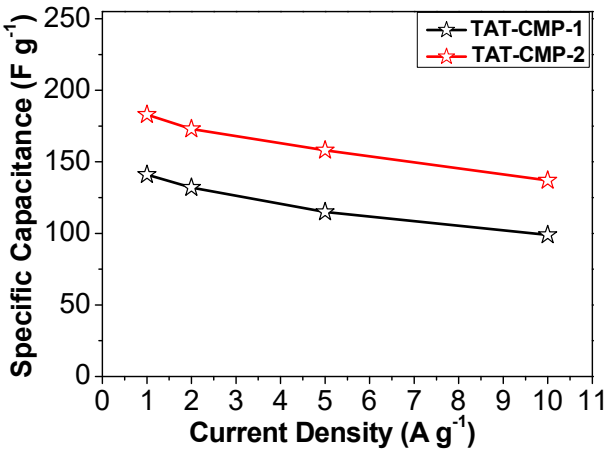

Figure S13. The specific capacitances calculated by the CP curves and current densities of **TAT-CMP-1** and **TAT-CMP-2.**

Table S2. Performance comparison of areal capacitances among various porous materials.

Materials	Capacitance gravimetric F g^{-1} (Conditions)	Normalized capacitance μF cm^{-2} (S_{BET}, m^2 g^{-1})	Reference
TAT-CMP-1	**141 (1 A g^{-1})**	**160 (88)**	**This Work**
TAT-CMP-2	**183 (1 A g^{-1})**	**173 (106)**	**This Work**
covalent organic frameworks	48 (0.1 A g^{-1})	4 (1124)	2
carbon nanotubes	98 (1 A g^{-1})	10 (988)	3
porous carbon nanosheets	128 (0.1 A g^{-1})	7 (1735)	4
carbon nanoparticles	84 (1 A g^{-1})	23 (365)	5
porous carbon materials	129 (10 A g^{-1})	20 (655)	6
mesoporous carbon	160 (1 A g^{-1})	14 (1161)	7
nitrogen-enriched porous carbons	166 (0.1 A g^{-1})	33 (500)	8

3. MALDI-TOF and NMR spectra

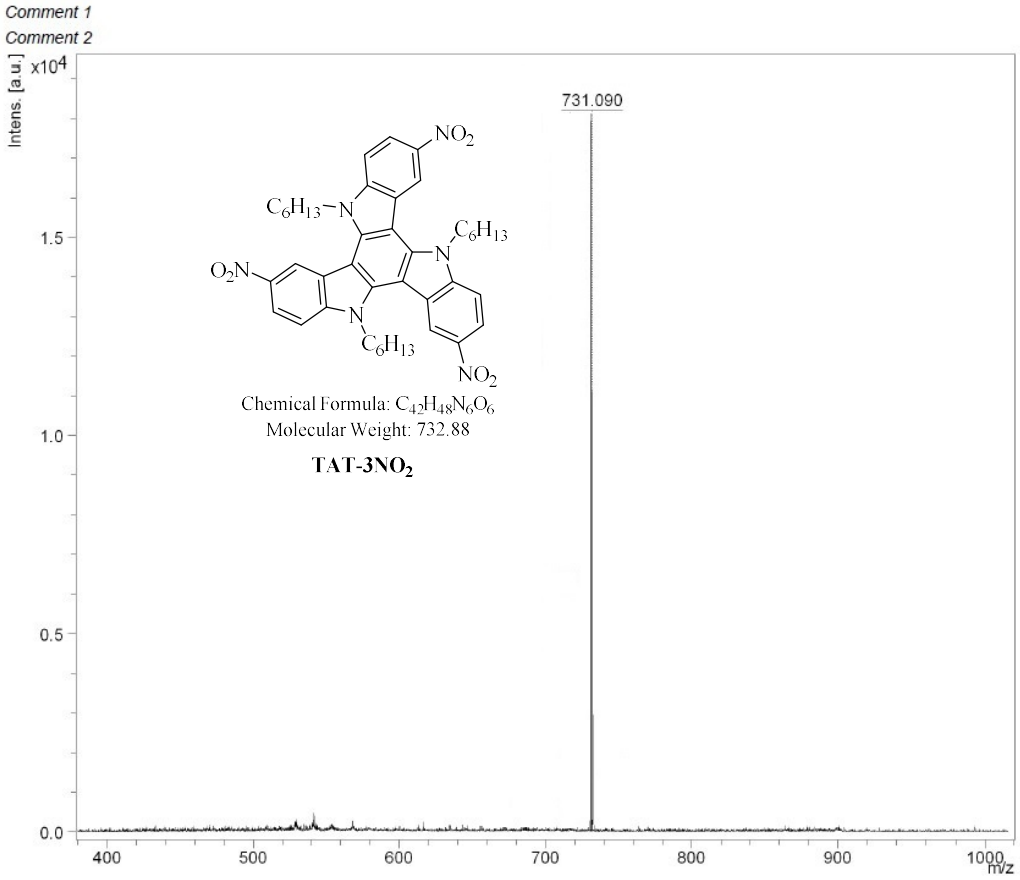

Figure S15. MALDI-TOF of **TAT-3NO$_2$**.

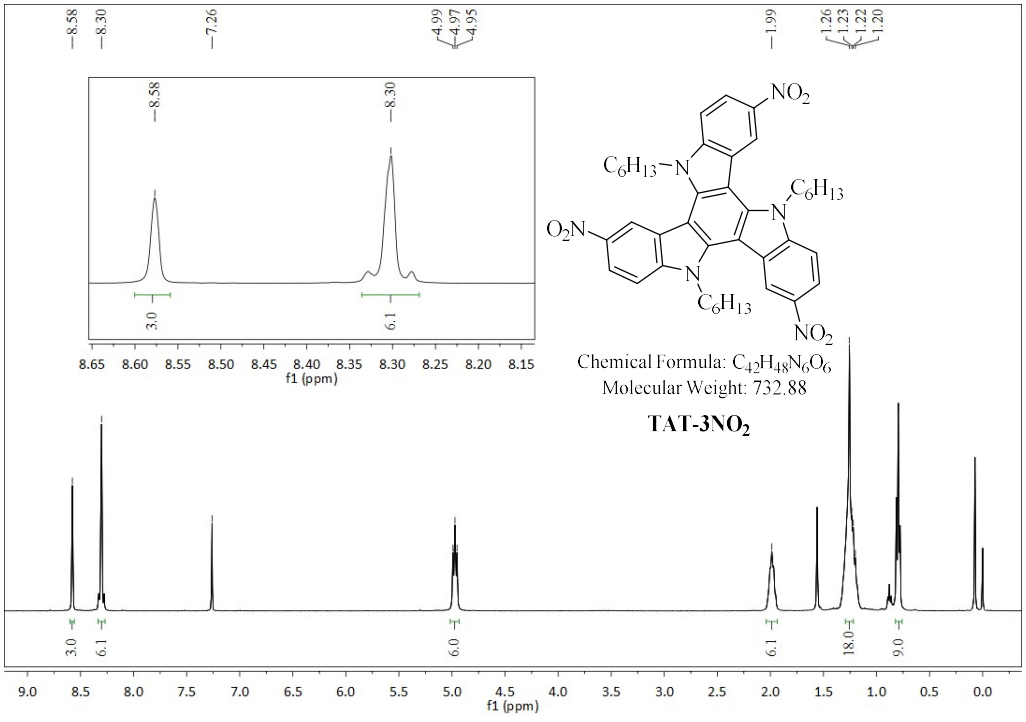

Figure S16. ^{1}H NMR of **TAT-3NO$_2$**.

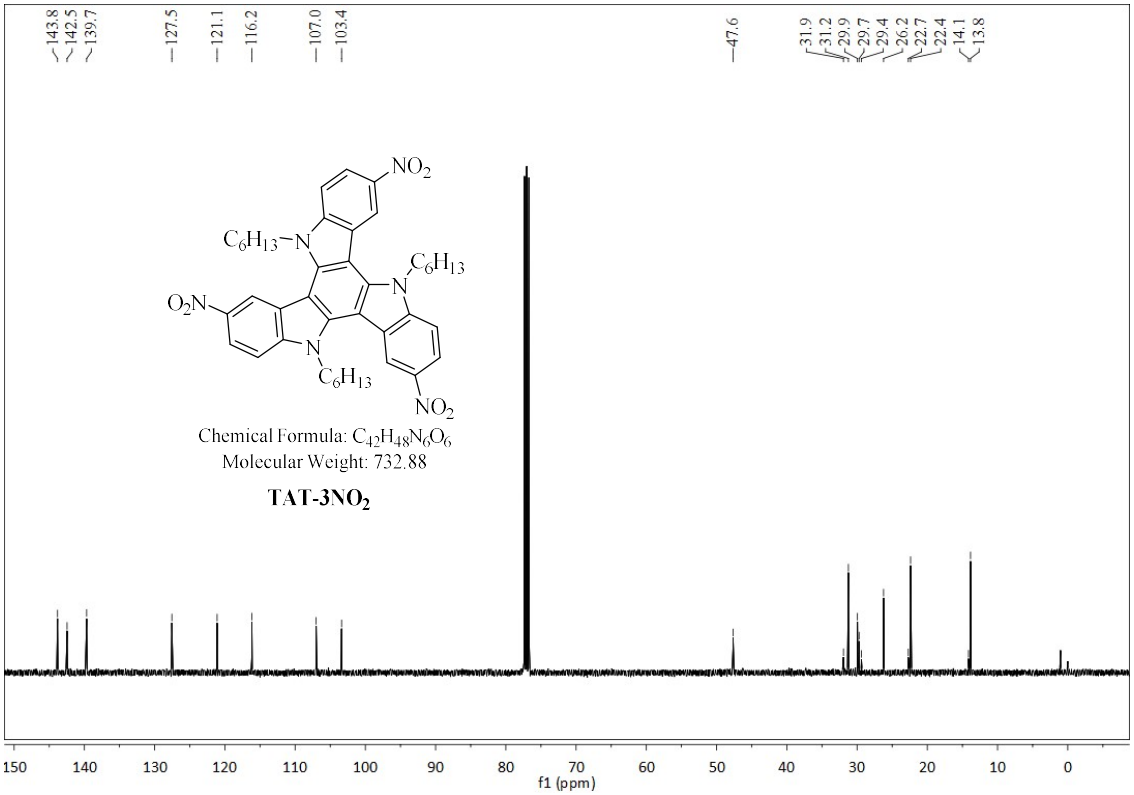

Figure S17. ^{13}C NMR of **TAT-3NO$_2$**.

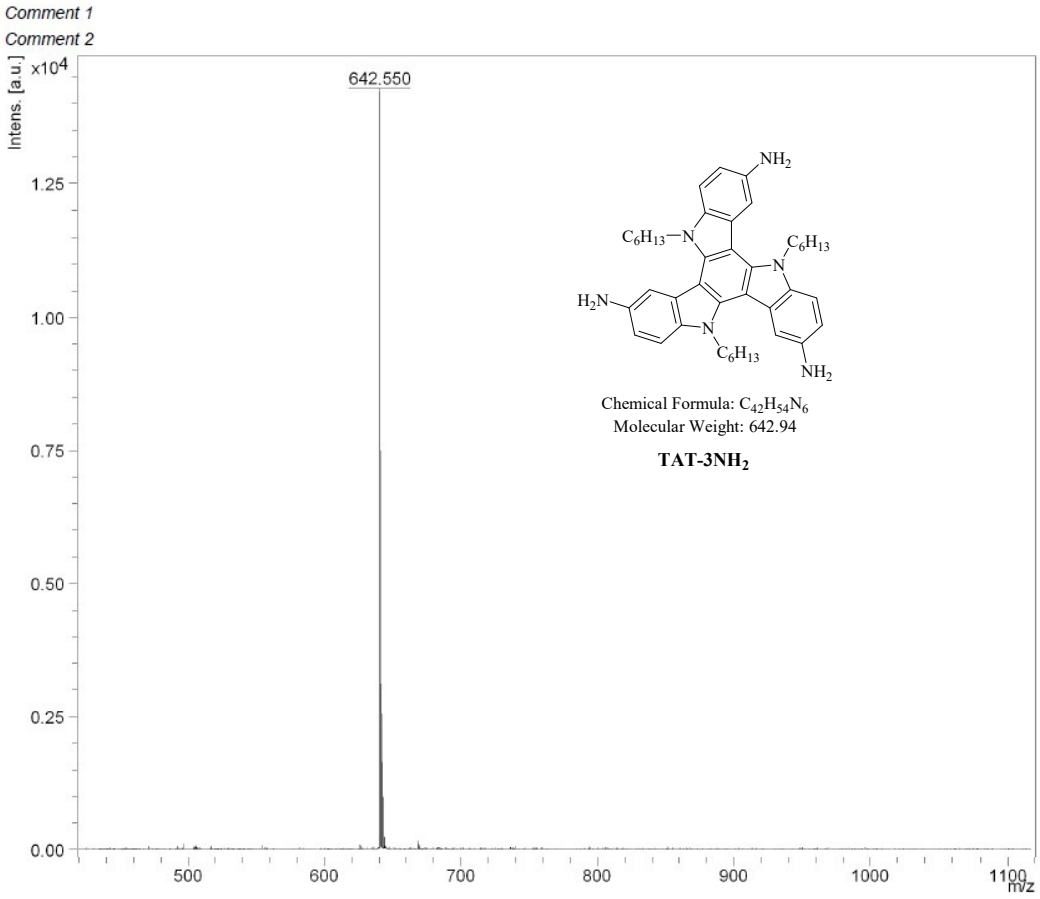

Figure S18. MALDI-TOF of **TAT-3NH$_2$**.

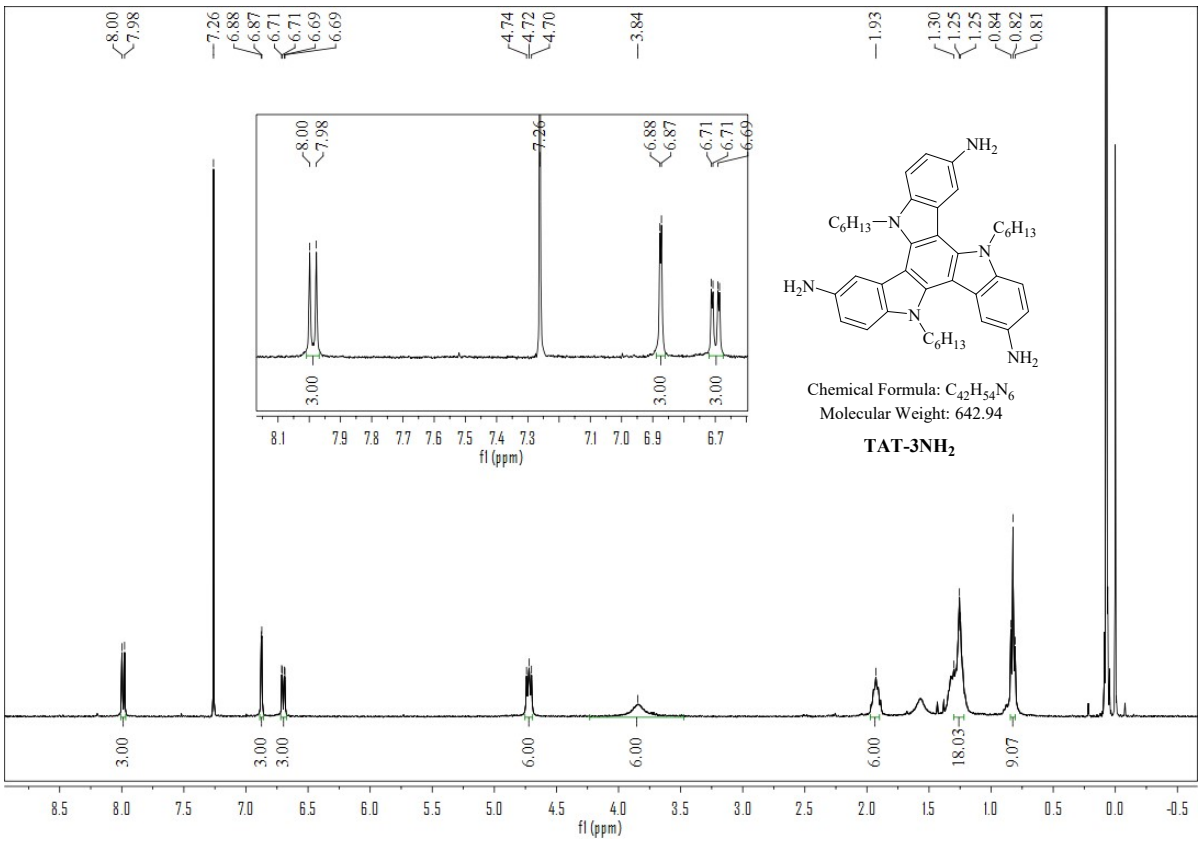

Figure S19. ^{1}H NMR of **TAT-3NH$_2$**.

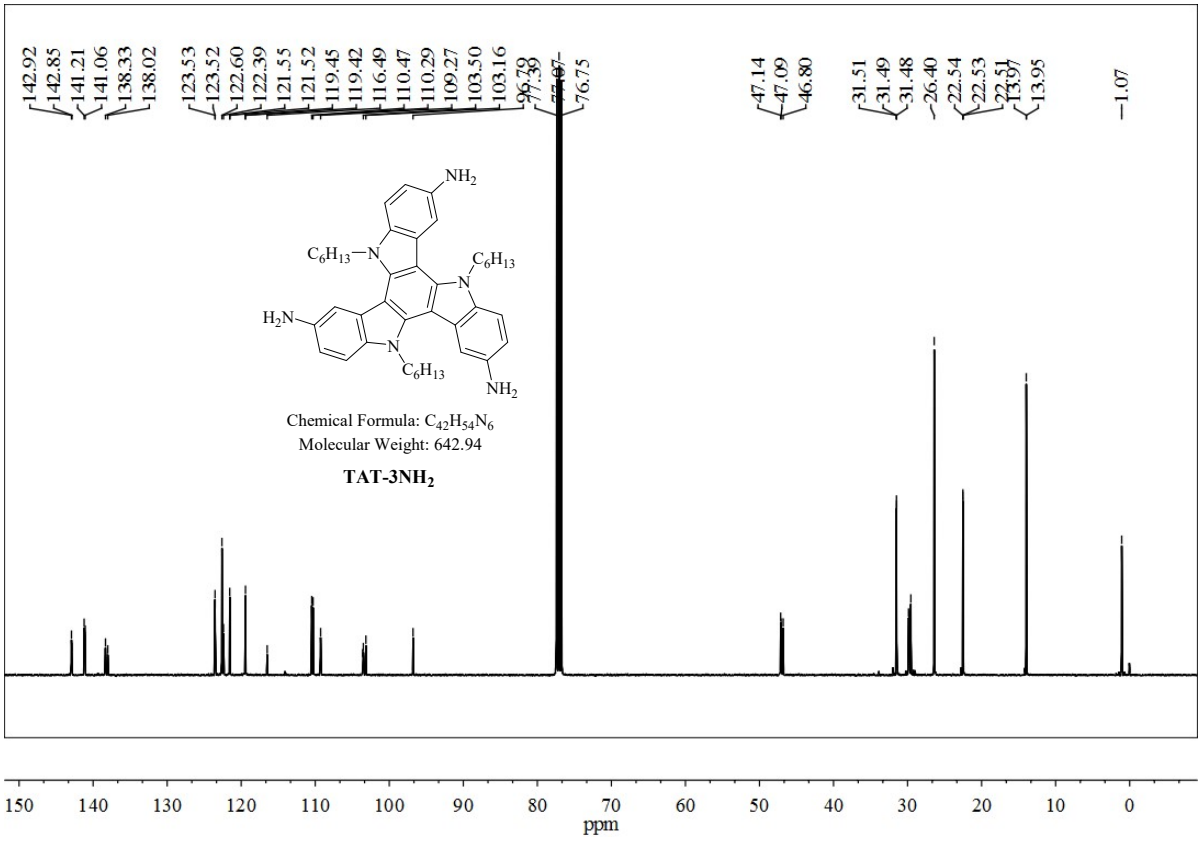

Figure S20. ^{13}C NMR of **TAT-3NH$_2$**.

4. References

1. X.-C. Li, C.-Y. Wang, Y. Wan, W.-Y. Lai, L. Zhao, M.-F. Yin and W. Huang, *Chem. Commun.*, 2016, **52**, 2748-2751.

2. C. R. DeBlase, K. E. Silberstein, T.-T. Truong, H. C. D. Abruña and W. R. Dichtel, *J. Am. Chem. Soc.*, 2013, **135**, 16821-16824.

3. Y. S. Yun, G. Yoon, K. Kang and H.-J. Jin, *Carbon*, 2014, **80**, 246-254.

4. X. Yu, J. Zhao, R. Lv, Q. Liang, C. Zhan, Y. Bai, Z.-H. Huang, W. Shen and F. Kang, *J. Mater. Chem. A*, 2015, **3**, 18400-18405.

5. L.-P. Lv, Z.-S. Wu, L. Chen, H. Lu, Y.-R. Zheng, T. Weidner, X. Feng, K. Landfester and D. Crespy, *RSC Adv.*, 2015, **5**, 50063-50069.

6. G. Xu, J. Han, B. Ding, P. Nie, J. Pan, H. Dou, H. Li and X. Zhang, *Green Chem.*, 2015, **17**, 1668-1674.

7. S. Zhang, A. Ikoma, K. Ueno, Z. Chen, K. Dokko and M. Watanabe, *ChemSusChem*, 2015, **8**, 1608-1617.

8. M. Zhong, E. K. Kim, J. P. McGann, S.-E. Chun, J. F. Whitacre, M. Jaroniec, K. Matyjaszewski and T. Kowalewski, *J. Am. Chem. Soc.*, 2012, **134**, 14846-14857.